Available online at http://scik.org
Commun. Math. Biol. Neurosci. 2019, 2019:26
https://doi.org/10.28919/cmbn/4136
ISSN: 2052-2541

PORTRAYING THE EFFECT OF SOURCE INFLUX ON INTERDEPENDENT CALCIUM AND INOSITOL $1,4,5-$TRISPHOSPHATE DYNAMICS IN CARDIAC MYOCYTE

NISHA SINGH* AND NEERU ADLAKHA

Applied Mathematics and Humanities Department,

Sardar Vallabhbhai National Institute of Technology, Ichchhanath, Surat, Gujarat 395007, India

Abstract. Calcium governs the most versatile and universal signaling mechanism in living systems which includes contraction of the cardiac tissues, information processing in the brain, release of digestive enzymes by the liver etc. High blood calcium leads to various diseases and problems like chronic fatigue and tiredness, poor memory, atherosclerosis, muscle aches and cramps, bone pain, poor sex drive, osteoporosis and broken bones, kidney stones and heart rhythm problems such as atrial fibrillation. Various investigators have been made on study of calcium signaling in cardiac myocyte to understand its mechanisms. But most of existing investigators have mainly focused on study of calcium signaling in cardiac myocyte without paying attention on interdependence of calcium signaling and inositol$-1;4;5$ trisphosphate (IP_3) signaling. In the present work, we have studied a mathematical model to understand the impact of source influx of calcium and maximum rate of production of IP_3 on these coupled signaling processes. This study suggests that maximum rate of production of IP_3 plays a more significant role in these coupled dynamics. Also, calcium and IP_3 shows a beautiful coordination with each other, which explains the role of IP_3 in calcium signaling in cardiac myocyte. Such studies will provide the better understanding of various factors involved in calcium signaling in cardiac myocyte, which as a result will be of great use to biomedical scientists for making protocols for various heart diseases.

Keywords: calcium signaling; coupling; IP_3; maximum rate of IP_3 production; source influx.

2010 AMS Subject Classification: 93A30.

*Corresponding author

E-mail address: nishasingh.maths@gmail.com

Received May 21, 2019

1. INTRODUCTION

Heart failure is a dynamic and diligent sickness, portrayed by diminished capacity of the heart to pump blood [1]. Heart failure remains a genuine medical problem all through the world. Nowadays the issue of heart failure is also common in young age people as well. Patients with heart failure experience the ill effects of the major problem and the accessible medications are frequently lacking. The exact components which prompt heart failure are yet not surely known. It is basic to comprehend the capacity of heart to manage heart related illnesses. The heart is in charge of the course of blood in the human body. Blood conveys supplements which are essential for the capacity and life of various organs. Additionally, blood retains the waste produced in the body [2]. Hence, legitimate blood circulation is important for keeping up structure and elements of various organs. The blood circulation is directed by systematic and rhythmic expansion and contraction of heart.

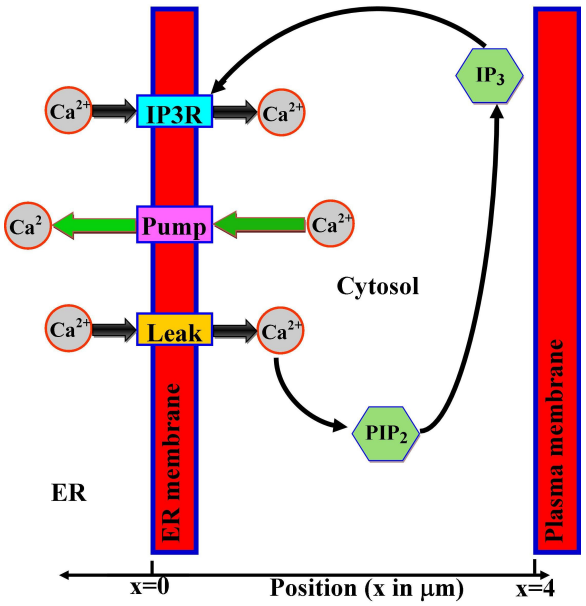

FIGURE 1. The mechanism of calcium (Ca^{2+}) and IP_3 dynamics in a cardiac myocyte including IP_3 receptor (IP_3R), *SERCA* pump and leak. The position $x = 0\ \mu m$ represents the position of the source influx of Ca^{2+} and $x = 4\ \mu m$ represents the position of IP_3 influx.

Cardiac myocytes are the cells present in the heart which are in charge of expansion and contraction of heart by a complex procedure which does the pumping of blood from heart to the circulatory framework. It is subsequently vital to comprehend the extension and compression system of cardiac myocytes. The centralization of calcium particles inside heart muscle cells assume a basic job in fortifying the constriction of heart amid the heartbeat. Intracellular Ca^{2+} dynamics which happens in cardiac myocyte for accomplishing the basic functions of heart is a complex process [3]. This particular intracellular Ca^{2+} dynamics is accomplished by different biophysical processes like diffusion, influx, rate of maximum production, source, leak and so on which occur in cardiac myocyte. Additionally, calcium is lethal to the cells consequently its overabundance can be destructive to the cell. The calcium regulation in the cell, happens through different biological processes which governs transition of the calcium. Subsequently, it is exceptionally important to understand how the intracellular calcium focus is overseen by different biological parameters and procedures [4].

A wealth of experimental data is available detailing elementary Ca^{2+} release events [5] and functional properties of the IP_3 receptors. Experiments are limited by protocol and therefore computational studies, across different spatial and temporal scales, are a significant and indispensable tool. Various attempts for the study of calcium regulation in other cells [6, 7, 8, 9, 10, 11, 12, 13, 14] are reported in the literature. Pathak *et al.* [15] have developed mathematical models to understand independent Ca^{2+} signaling process in cardiac myocyte. But they have not considered the impact of IP_3 dynamics in their model. But some experimental studies [16, 17, 18] as well as theoretical investigations [19, 20, 21] have shown the importance of other ions on calcium dynamics in cell. Also, Li and Rinzel [22] have reduced the nine-variable De Young-Keizer model [23] for Ca^{2+} dynamics mediated by IP_3 receptor (IP_3R) in endoplasmic reticulum (ER) membrane to a two-variable system. Myocytes can distinguish simultaneous local and global Ca^{2+} signals involved in contractile activation from those targeting gene expression [24]. Hohendanner *et al.* [25] have discussed the state of knowledge regarding the origin and the physiological implications of Ca^{2+} transients in different cardiac cell types (adult atrial and ventricular myocytes) as well as experimental and mathematical approaches to study Ca^{2+} and IP_3 dynamics in the cytosol. In the present work a systematic effort has been

made to study a mathematical model to understand the dependence of Ca^{2+} and IP_3 dynamics on each other and also, the effect of source of Ca^{2+} and maximum rate of production of IP_3 on cell signaling process. The present model is used to explain intracellular calcium signaling in cardiac myocyte including IP_3 dynamics. A successful model should be able to predict and explain functional properties involved in the process of calcium signaling [26].

2. MAIN RESULTS

2.1. Calcium and IP_3 dynamics model. The underlying mechanism of coupled Ca^{2+} and IP_3 dynamics in a cardiac myocyte as shown in FIGURE 1 leads to a Ca^{2+} and IP_3 dynamic mathematical model. FIGURE 1 illustrates all the influxes and outfluxes of this mechanism. The arrows in FIGURE 1 demonstrates the pathway of Ca^{2+} and IP_3 flow in cytosol of cardiac myocyte. Due to the leak attached to the ER membrane, free Ca^{2+} ions leaks in the cytosol from ER which breaks phosphatidylinositol 4,5-bisphosphate(PIP_2) to release IP_3 which then gets bind with IP_3 receptor (IP_3R) and opens the receptor gate to facilitate diffusion of free Ca^{2+} ions from ER to cytosol. Now, when the concentration of free Ca^{2+} ions increase in cytosol then *SERCA* pump comes into picture. It flush out the excess Ca^{2+} ions from cytosol to ER to maintain the background concentration of Ca^{2+} in cytosol. Again the whole process takes place and so on. The cyclic and dynamic process leads to few reaction-diffusion equations. The reaction-diffusion equations for Ca^{2+} and IP_3 are given by [27],

$$\frac{\partial [Ca^{2+}]}{\partial t} = D_c \nabla^2 [Ca^{2+}] + \frac{J_{IPR} - J_{SERCA} + J_{Leak}}{F_c}, \tag{1}$$

where $[Ca^{2+}]$ is the concentrations of Ca^{2+} in the cytosol, D_c is the diffusion coefficient of cytosolic calcium and various flux terms are given by [27],

$$J_{IPR} = V_{IPR} m^3 h^3 ([Ca^{2+}]_e - [Ca^{2+}]), \tag{2}$$

$$J_{Leak} = V_{Leak} ([Ca^{2+}]_e - [Ca^{2+}]), \tag{3}$$

$$J_{SERCA} = V_{SERCA}\frac{[Ca^{2+}]^2}{K_{SERCA}^2 + [Ca^{2+}]^2}, \tag{4}$$

where J_{IPR}, J_{Leak} and J_{SERCA} are the flux terms for IP_3R, leak and *SERCA* pump respectively. Also, $[Ca^{2+}]_e$ is the concentrations of Ca^{2+} in the ER. V_{IPR} and V_{Leak} are flux rate constants of IP_3 receptor and leak respectively. Whereas, V_{SERCA} is the maximum *SERCA* pump rate. Here, Michaelis constant for *SERCA* pump is denoted by K_{SERCA}. In this formulation, F_c and F_e are the volume fractions, relative to total cell volume, of the cytosol and ER, respectively (with $F_c + F_e = 1$). The Li-Rinzel model [22] , however, utilizes time scale arguments to eliminate two of the three binding reactions, replacing them with the equilibrium equation [27],

$$m = \frac{[IP_3]}{[IP_3] + K_{IP_3}}\frac{[Ca^{2+}]}{[Ca^{2+}] + K_A}, \tag{5}$$

where $[IP_3]$ is the concentration of IP_3 in cytosol. The variable h represents the fraction of subunits not yet inactivated by Ca^{2+} is given by [27],

$$h = \frac{K_{Inh}}{K_{Inh} + [Ca^{2+}]}, \tag{6}$$

Here, activating IP_3 binding site dissociation constant, activating Ca^{2+} binding site dissociation constant and inhibiting Ca^{2+} binding site dissociation constant are denoted by K_{IP_3}, K_A and K_{Inh} respectively. Also, shown in FIGURE 1 are IP_3 production and degradation pathways. The reaction-diffusion equation for the cytosolic IP_3 concentration ($[IP_3]$) is given by [27],

$$\frac{\partial [IP_3]}{\partial t} = D_i \nabla^2 [IP_3] + \frac{J_{Production} - \lambda (J_{Kinase} + J_{Phosphatase})}{F_c}, \tag{7}$$

where D_i is the diffusion coefficient of IP_3. All the flux terms involved in IP_3 dynamics are given by [27],

$$J_{Production} = V_{Production}\frac{[Ca^{2+}]^2}{[Ca^{2+}]^2 + K_{Production}^2}, \tag{8}$$

$$J_{Kinase} = (1-\theta)V_1 \frac{[IP_3]}{[IP_3]+2.5} + \theta V_2 \frac{[IP_3]}{[IP_3]+0.5}, \tag{9}$$

$$J_{Phosphatase} = V_3 \frac{[IP_3]}{[IP_3]+30}, \tag{10}$$

Here, $J_{Production}$, J_{Kinase} and $J_{Phosphatase}$ are fluxes for IP_3 production, Kinase and Phosphatase respectively. Also, $V_{Production}$ is maximum IP_3 production and $K_{Production}$ is Michaelis constant for Ca^{2+} activation. Whereas, V_1 denotes maximum rate constant at low Ca^{2+}, V_2 is maximum rate constant at high Ca^{2+} and V_3 is maximum rate constant of phosphatase. The parameter values used in these equations are taken from Xenopus oocytes [28], but because the overall rate was found to be too slow, we have scaled the entire degradation rate by an adjustable parameter, λ which is scaling factor. The Ca^{2+} dependence of the 3-kinase degradation pathway is described by a Hill function [27],

$$\theta = \frac{[Ca^{2+}]}{[Ca^{2+}]+0.39}, \tag{11}$$

The analysis of the complete model is not possible using basic phase plane techniques. However, in a whole-cell model (i.e. where the diffusion terms are eliminated), the $[Ca^{2+}]_e$ equation can be eliminated using the conservation relation for the total cellular Ca^{2+} concentration ($[Ca^{2+}]_T$) [27],

$$[Ca^{2+}]_T = F_c[Ca^{2+}] + F_e[Ca^{2+}]_e, \tag{12}$$

This allows the model to be reduced to the three variables $[Ca^{2+}]$, $[IP_3]$, and h [29]. Here, it is assumed that all the calcium buffers are fast, immobile and unsaturated [30, 31]. Thus, the calcium buffering is included implicitly in this model by treating all calcium fluxes as explicit fluxes. Now, this model is formulated to study Ca^{2+} and IP_3 dynamics and role of source influx on these dynamics in one dimensional unsteady state case in the next section.

2.2. One dimensional model to study Ca^{2+} and IP_3 dynamics. The calcium diffusion in cardiac myocyte in the presence of IP_3 dynamics for one dimensional unsteady state case is given by [27],

$$\frac{\partial [Ca^{2+}]}{\partial t} = D_c \frac{\partial^2 [Ca^{2+}]}{\partial x^2} + \frac{J_{IPR} - J_{SERCA} + J_{Leak}}{F_c}, \tag{13}$$

And IP_3 diffussion in cardiac myocyte in the presence of Ca^{2+} dynamics for one dimensional unsteady state case is given by [27],

$$\frac{\partial [IP_3]}{\partial t} = D_i \frac{\partial^2 [IP_3]}{\partial x^2} + \frac{J_{Production} - \lambda (J_{Kinase} + J_{Phosphatase})}{F_c}, \tag{14}$$

The initial and boundary conditions governing the Ca^{2+} and IP_3 diffusion process are given by [32, 33, 34],

(i) Initial condition

$$[Ca^{2+}]_{t=0} = 0.1\ \mu M, \tag{15}$$

$$[IP_3]_{t=0} = 0.16\ \mu M, \tag{16}$$

(ii) Boundary condition

$$\lim_{x \to 0} \left(-D_c \frac{\partial [Ca^{2+}]}{\partial x} \right) = \sigma, \tag{17}$$

$$\lim_{x \to 4} [Ca^{2+}] = [Ca^{2+}]_{\infty} = 0.1\ \mu M, \tag{18}$$

Also, the boundary conditions governing IP_3 dynamics in this model are derived from Brown *et al.* [32]. They have experimentally derived $3-D$ geometry displayed time-dependent behavior of the IP_3, therefore following boundary condition used was the polynomial fit.

$$\lim_{x\to 4}[IP_3] = 0.1882(t)^6 + 1.3121(t)^5 + 3.5391(t)^4 + 4.5312(t)^3$$

$$+2.5893(t)^2 + 0.3648(t) + 0.1691 \leq 3, \tag{19}$$

$$\lim_{x\to 0}[IP_3] = 3\ \mu M; \qquad t > 0, \tag{20}$$

where, t denotes time.

The model equations (13)–(20) are solved numerically using Crank Nicholson Method Scheme. This scheme is very useful in those cases where solution needs to be time perfect. This method is implicit and unconditionally stable. Under this scheme the time derivative is approximated using backward difference formula and space derivative is approximated using the average of second order central difference formula evaluated at current and previous time steps [35],

$$\frac{\phi_i^j - \phi_i^{j-1}}{k} = \frac{1}{2}\left\{\frac{\phi_{i+1}^j - 2\phi_i^j + u_{i-1}^j}{h^2} + \frac{\phi_{i+1}^{j-1} - 2\phi_i^{j-1} + \phi_{i-1}^{j-1}}{h^2}\right\}, \tag{21}$$

Since this method is an implicit method it requires solving a system of equations at each time step. Then the resulting system provides simultaneous algebraic equations for unknown nodal concentrations. Gaussian elimination method has been employed to solve the resulting equations for each time step.

3. RESULTS AND DISCUSSION

This section investigates the interdependence of Ca^{2+} and IP_3 dynamics inside the cardiac myocyte. Inside the cardiac myocyte, the IP_3 concentration and Ca^{2+} concentration are strongly interdependent. Therefore, we have simulated the dependence of Ca^{2+} and IP_3 on each other as well as we have tried to understand role of various parameters like source of Ca^{2+} (σ) and maximum rate of production of IP_3 $(V_{Production})$ on this interdependence of Ca^{2+} and IP_3. The parameters used for the computation of numerical results are given in TABLE 1 or in the text (where needed). To facilitate our discussion, all calculations utilize the standard model parameters in TABLE 1, except where noted otherwise.

TABLE 1. Standard parameters for Ca^{2+} and IP_3 signaling.

Parameters	Values [27]	Parameters	Values [27]
V_{IPR}	$8.5\ s^{-1}$	V_{Leak}	$0.01\ s^{-1}$
K_{IP_3}	$0.15\ \mu M$	K_A	$0.8\ \mu M$
V_{SERCA}	$0.65\ \mu M/s$	K_{SERCA}	$0.4\ \mu M$
K_{Inh}	$1.8\ \mu M$		
$V_{Production}$	$0.075\ \mu M/s$	$K_{Production}$	$0.4\ \mu M$
V_1	$0.001\ \mu M/s$	V_2	$0.005\ \mu M/s$
V_3	$0.02\ \mu M/s$	λ	30
D_c	$16\ \mu m^2/s$	D_e	$16\ \mu m^2/s$
D_i	$283\ \mu m^2/s$	$[Ca^{2+}]_T$	$1.7\ \mu M$
F_c	0.83	F_e	0.17

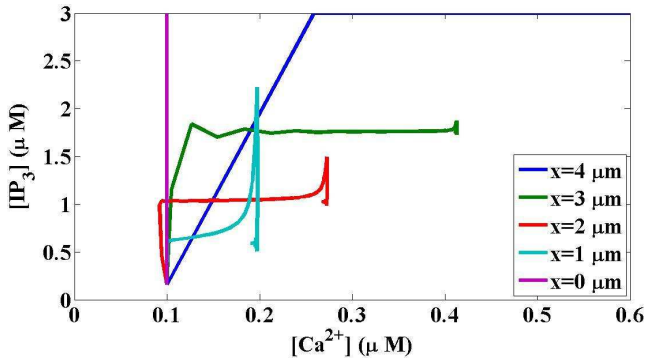

FIGURE 2. Ca^{2+} and IP_3 concentration profile in cardiac myocyte with respect to each other at different positions x varies from $x = 0\ \mu m$ to $x = 4\ \mu m$. Here, $\sigma = 10\ \rho A$ and $V_{Production} = 0.075\ \mu M/s$.

The dependence of Ca^{2+} and IP_3 concentrations on each other at different positions (x) in the cytosol of cardiac myocyte is shown in FIGURE 2. Initially, it satisfied the boundary condition

at lowest value of x. Furthermore, at $x = 1\ \mu m$, the $[IP_3]$ is rapidly increases and then at particular value, it becomes steady state after that at the certain value, $[Ca^{2+}]$ becomes fixed and the IP_3 concentration again increase suddenly (see in FIGURE 2). Also, we found that, at all value of x except $x = 0\ \mu m$ which is source of Ca^{2+} and $x = 4\ \mu m$ which is source of IP_3, the concentration of IP_3 suddenly goes down and it fluctuates and becomes steady state and at the same time Ca^{2+} concentration has been slightly decreases. Same behavior but higher values of IP_3 in the variation of Ca^{2+} and IP_3 concentration has been found at $x = 2\ \mu m$ and $x = 3\ \mu m$ but saturation range is longer as compare to lower values. It is observed that Ca^{2+} and IP_3 increases proportionally but after some time IP_3 concentration becomes steady while Ca^{2+} concentration increases. Thereafter, when Ca^{2+} concentration becomes steady then we can observe a peak in IP_3 concentration which rises very quickly and falls. This peak of IP_3 concentration is due to the uncaging of IP_3 ions in cytosol. These observation clearly represent the nonlinear interdependence of $[Ca^{2+}]$ and $[IP_3]$. Also, it validates the strong dependence of $[Ca^{2+}]$ on $[IP_3]$ and vice versa. These observations in FIGURE 2 indicates that the present mathematical model is more realistic as compared to Pathak *et al.* [15, 36] as their model lacks the important role of IP_3 in the dynamics of Ca^{2+} in cardiac myocyte.

FIGURE 3 shows the dependence of Ca^{2+} and IP_3 concentrations on each other at different positions in the cytosol for $\sigma = 6\ \rho A$ (solid lines), $12\ \rho A$ (dashed lines), $18\ \rho A$ (dotted lines) and (a) $V_{Production} = 0.025\ \mu M/s$, (b) $V_{Production} = 0.050\ \mu M/s$, (c) $V_{Production} = 0.075\ \mu M/s$, (d) $V_{Production} = 0.100\ \mu M/s$. Here, σ represents the source of Ca^{2+} and $V_{Production}$ represent maximum rate of IP_3 production. But FIGURE 2, shows the variation of Ca^{2+} and IP_3 concentrations at particular source of Ca^{2+} and fixed value of maximum rate of IP_3 production. Now, we can see that the effect of different values of source influx (σ) of Ca^{2+} on interdependent Ca^{2+} and IP_3 concentrations in FIGURE 3 at fixed maximum rate of IP_3 production $(V_{Production})$. It's observed that, the same behavior has been found as FIGURE 2 but a quantitative difference can be clearly observed in FIGURE 3. This graphs shows the interdependence of Ca^{2+} and IP_3 concentration is slightly affected by the increase in the source influx of Ca^{2+} i.e. σ and all the fixed values of $V_{Production}$ (see FIGURE 3(a) to 3(d)). We can observe that all the same colored lines which are parallel to x-axis are slightly away from each other showing

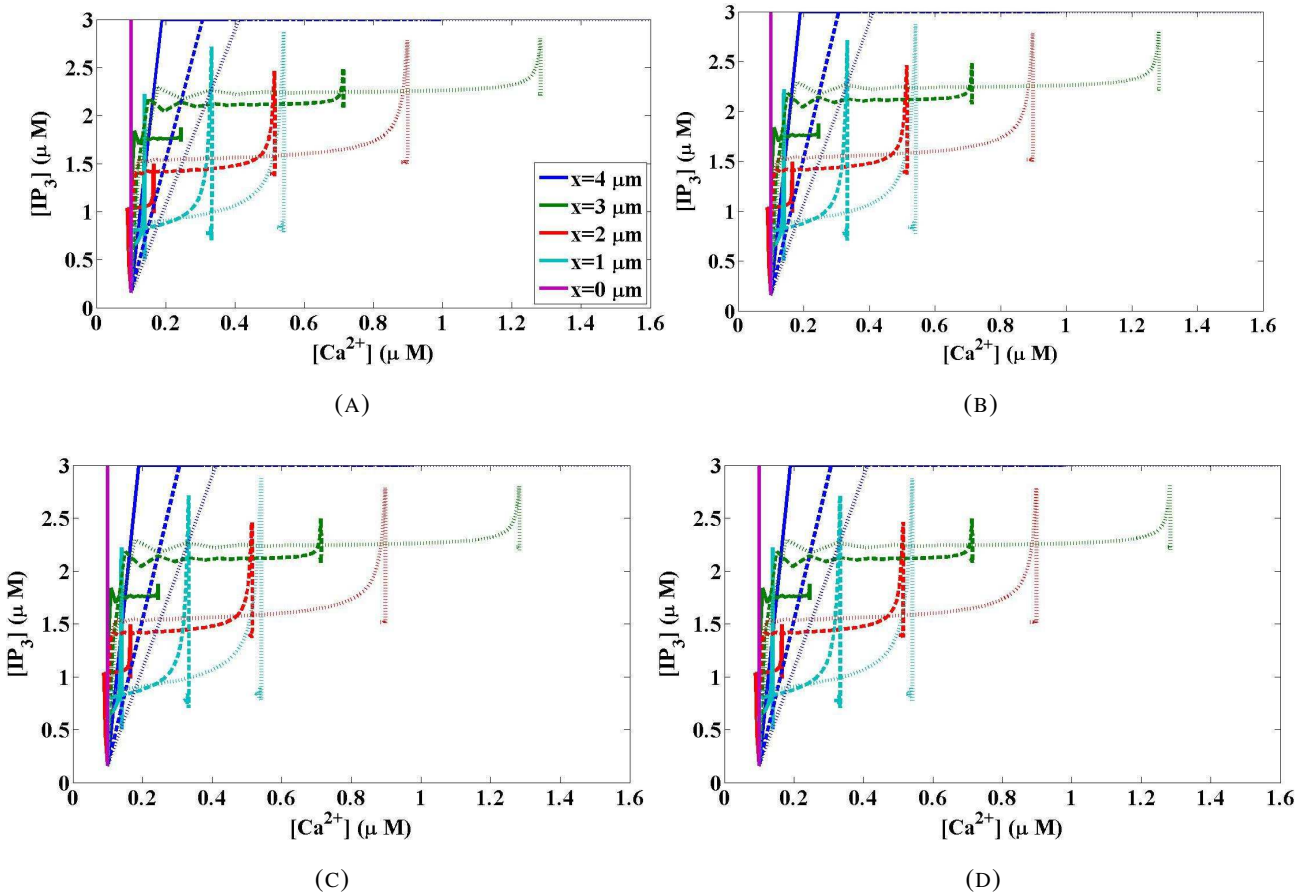

FIGURE 3. Ca^{2+} and IP_3 concentration profile in cardiac myocyte with respect to each other at different positions x for $\sigma = 6\ \rho A$ (solid lines), $12\ \rho A$ (dashed lines), $18\ \rho A$ (dotted lines) and (a) $V_{Production} = 0.025\ \mu M/s$, (b) $V_{Production} = 0.050\ \mu M/s$, (c) $V_{Production} = 0.075\ \mu M/s$, (d) $V_{Production} = 0.100\ \mu M/s$.

increase in IP_3 concentration due to increase in σ at different positions (x) in the cytosol of cardiac myocyte. And the value of Ca^{2+} concentration at which this interdependence becomes steady is also increases with the increase of value of σ. But from FIGURE 3(a), 3(b), 3(c) and 3(d), we have observed that at all fixed values of $V_{Production}$ the behaviour and values of the interdependent graphs is almost same. This shows that at fixed value of $V_{Production}$ if source influx of Ca^{2+} is varied then it will not be able to make any qualitative as well as quantitative difference in the dynamics of interdependent Ca^{2+} and IP_3 in cardiac myocyte.

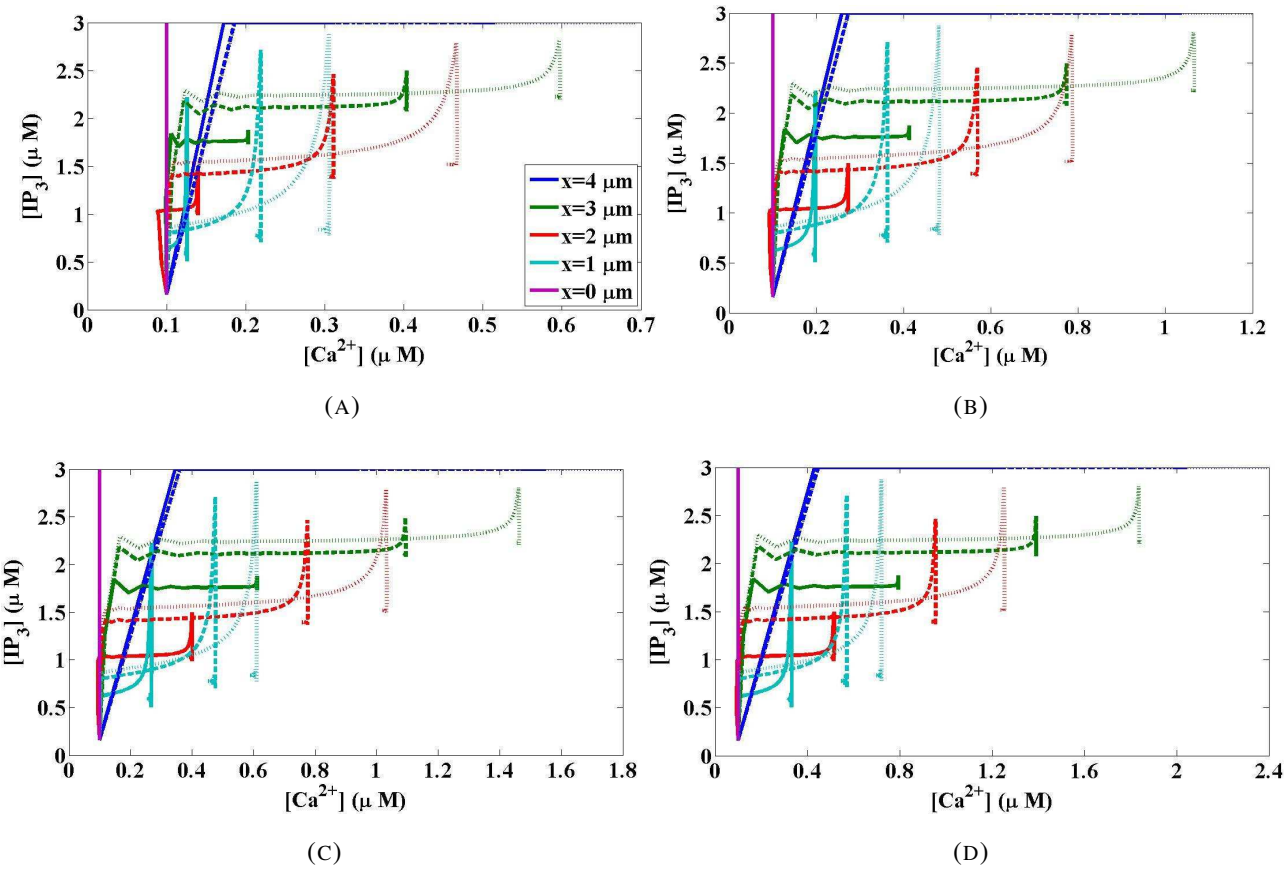

FIGURE 4. Ca^{2+} and IP_3 concentration profile in cardiac myocyte with respect to each other at different positions x for $V_{Production} = 0.06\ \mu M/s$ (solid lines), $0.12\ \mu M/s$ (dashed lines), $0.18\ \mu M/s$ (dotted lines) and (a) $\sigma = 5\ \rho A$, (b) $\sigma = 10\ \rho A$, (c) $\sigma = 15\ \rho A$, (d) $\sigma = 20\ \rho A$.

Bartlett *et al.* [37] recently showed how differential regulation of intermediate steps in IP_3 creation can have a significant impact on calcium dynamics. Inspired by this we have discussed the effect of maximum rate of IP_3 ions production $(V_{Production})$ on Ca^{2+} and IP_3 concentrations. FIGURE 4 shows the dependence of Ca^{2+} and IP_3 concentrations on each other at different (x) positions in the cytosol for $V_{Production} = 0.06\ \mu M/s$ (solid lines), $0.12\ \mu M/s$ (dashed lines), $0.18\ \mu M/s$ (dotted lines) and (a) $\sigma = 5\ \rho A$, (b) $\sigma = 10\ \rho A$, (c) $\sigma = 15\ \rho A$, (d) $\sigma = 20\ \rho A$. Also, this graphs shows the interdependent Ca^{2+} and IP_3 concentration is quite affected by the increase in the $V_{Production}$ i.e. maximum rate of production of IP_3 ions. We can observe that all the same colored lines which are parallel to y-axis are quite away from each other

showing increase in Ca^{2+} concentration due to increase in $V_{Production}$ at different positions (x) in the cytosol of cardiac myocyte. From FIGURE 4(a), 4(b), 4(c) and 4(d) it is observed that at all the fixed values of σ, when $V_{Production}$ is varied a quantitative significant change is seen. Also, at higher fixed value of σ the point of steady state is also attained at a higher value of Ca^{2+} concentration. As compared to FIGURE 3, it is clearly validated that FIGURE 4 shows much significant quantitative change in the interdependent Ca^{2+} and IP_3 concentration. This observation confirms that the impact of maximum rate of IP_3 production $(V_{Production})$ is remarkable in the coupled dynamics of Ca^{2+} and IP_3 in cardiac myocyte.

From these results, we can say that the Ca^{2+} and IP_3 concentrations are strongly dependent on each other as well as it is affected by various parameters like increasing the source of Ca^{2+} and maximum rate of production of IP_3 ions. But maximum rate of production of IP_3 $(V_{Production})$ is a parameter which can control this dynamics very well. By varying the value of $V_{Production}$ the uneven Ca^{2+} and IP_3 concentration due to which diseases like atherosclerosis (hardening of the arteries) happen can be treated. Atherosclerosis is the main cause of heart disease. It occurs because of calcium build-up in the blood vessels resulting in hard and narrow arteries. This then leads to problems such as blood flow obstruction and heart issues [38]. Above results conclude that IP_3 plays a vital role in calcium dynamics. As IP_3 concentration increases, Ca^{2+} concentration also increases at first then gradually becomes steady. Also, maximum rate of production of IP_3 $(V_{Production})$ is able to influence the interdependence more than source of calcium (σ) because when Ca^{2+} ion are release from the source of calcium then maximum amount of ions get attached with proteins in cytosol which decreases the amount of free Ca^{2+} in the cytosol of the cell. Whereas when maximum rate of production of IP_3 $(V_{Production})$ is increased then the releases IP_3 not only increase the amount of IP_3 in cytosol but it binds with the mouth of IP_3Rs to open them and facilitate the influx of Ca^{2+} ions from ER to cytosol. This results in overall increase in the concentration of the coupled dynamics which can be observed from FIGURE 4. In various models given in literature [15, 36, 39] they have excluded the role of IP_3, but many experimental works [23, 40, 41, 42] as well as theoretical works [6, 10, 19, 21] have shown the importance of IP_3 dynamics in calcium dynamics of cell. Sneyd *et al.* [21] have shown that the response to an artificial applied pulse of IP_3 in two types of cell. They have found

that long period Ca^{2+} dynamics in pancreatic acinar cells depends on IP_3 concentration but in airway smooth muscle, short term Ca^{2+} dynamics do not depend on IP_3 concentration. Also, Manhas *et al.* [10] have recently predicted that calcium-dependent production and degradation of IP_3 is a key mechanism for intracellular calcium dynamics in pancreatic acinar cells. So motivated by these works, we have studied a mathematical model to understand effect of IP_3 dynamics on intracellular Ca^{2+} dynamics and vice versa in cardiac myocyte, which describes the properties of elemental calcium release events in the presence of IP_3.

4. CONCLUSION

In this work, we have studied the interdependence of Ca^{2+} and IP_3 dynamics in cardiac myocyte. In which we have obtained the significant influence of source of Ca^{2+} and maximum rate of production of IP_3 ions on Ca^{2+} and IP_3 concentration dynamics. This model shows that, the variation on Ca^{2+} concentration and IP_3 concentration is affected by the source influx of Ca^{2+} (σ) as well as maximum rate of production of IP_3 $V_{Production}$. Also, it is observed that Ca^{2+} source influx has a very minute influence on IP_3 dynamics but on the other hand maximum rate of IP_3 production $(V_{Production})$ has quit significant impact on coupled Ca^{2+} and IP_3 dynamics. That is, both IP_3 production and diffusion are significant elements of the calcium dynamics in cardiac myocytes. The physical behaviour shown by the results matches with the behaviour observed in experimental investigations [27, 43]. These findings suggest that, Ca^{2+} and IP_3 concentration in cardiac myocyte can be effectively controlled by maximum rate of IP_3 production $(V_{Production})$ and it is important parameters during the modeling of treatment for heart diseases like atherosclerosis and heart rhythm problems such as atrial fibrillation.

ACKNOWLEDGEMENTS

The authors are thankful to the Department of Biotechnology, New Delhi, India for providing support in the form of Bioinformatics Infrastructure Facility for carrying out this work.

Conflict of Interests

The author(s) declare that there is no conflict of interests.

REFERENCES

[1] T. A. McDonagh, R. S. Gardner, A. L. Clark, and H. Dargie, Oxford textbook of heart failure. Oxford University Press, 2011.

[2] N. Weisleder, M. Brotto, S. Komazaki, Z. Pan, X. Zhao, T. Nosek, J. Parness, H. Takeshima, and J. Ma, Muscle aging is associated with compromised Ca^{2+} spark signaling and segregated intracellular Ca^{2+} release, J. Cell Biol., 174 (2006),639–645.

[3] D. M. Bers and T. A. O. Guo, Calcium signaling in cardiac ventricular myocytes, Ann. N. Y. Acad. Sci. , 1047 (2005), 86–98.

[4] E. Neher, Concentration profiles of intracellular calcium in the presence of a diffusible chelator, Exp. Brain Res., 14 (1986), 80–96.

[5] S. Dasgupta, G. D. Bader, and S. Goyal, Single-Cell RNA Sequencing: A New Window into Cell Scale Dynamics, Biophys. J., 115 (2018), 429–435.

[6] G. Dupont and A. Goldbeter, One-pool model for Ca^{2+} oscillations involving Ca^{2+} and inositol $1,4,5-$trisphosphate as co-agonists for Ca^{2+} release, Cell Calcium, 14 (1993), 311–322.

[7] A. Jha and N. Adlakha, Analytical solution of two dimensional unsteady state problem of calcium diffusion in a neuron cell, J. Med. Imaging Health Inform., 4 (2014), 547–553.

[8] B. Jha, A. Neeru, and M. Mehta, Analytic Solution of Two Dimensional Advection Diffusion Equation Arising In Cytosolic Calcium Concentration Distribution, Int. Math. Forum, 7 (2012), 135–144.

[9] M. Kotwani, N. Adlakha, and M. N. Mehta, Numerical model to study calcium diffusion in fibroblasts cell for one dimensional unsteady state case, Appl.Math. Sci., 6 (2012), 5063–5072.

[10] N. Manhas, J. Sneyd, and K. R. Pardasani, Modelling the transition from simple to complex Ca^{2+} oscillations in pancreatic acinar cells, J. Biosci., 39 (2014), 463–484.

[11] S. Panday and K. R. Pardasani, Finite element model to study effect of advection diffusion and Na^{+}/Ca^{2+} exchanger on Ca^{2+} distribution in Oocytes, J. Med. Imaging Health Inform., 3 (2013), 374–379.

[12] J. Sneyd and J. Sherratt, On the propagation of calcium waves in an inhomogeneous medium, SIAM J. Appl. Math., 57 (1997), 73–94.

[13] S. Tewari and K. R. Pardasani, Finite difference model to study the effects of Na^{+} influx on cytosolic Ca^{2+} diffusion, WorldA-cademy of Science, Eng. Technol., 15 (2008), 670–675.

[14] A. Tripathi and N. Adlakha, Finite volume model to study calcium diffusion in neuron cell under excess buffer approximation, Int. J. Math. Sci. Engg. Appls., 5 (2011), 437–447.

[15] K. B. Pathak and N. Adlakha, Finite Element Model to Study One Dimensional Calcium Dyanmics in Cardiac Myocytes, J. Multiscale Model., 6 (2015), 1550003.

[16] C.-h. Luo and Y. Rudy, A dynamic model of the cardiac ventricular action potential. II. Afterdepolarizations, triggered activity, and potentiation, Circulation Res., 74 (1994), 1097–1113.

[17] A. Michailova, F. DelPrincipe, M. Egger, and E. Niggli, Spatiotemporal Features of Ca^{2+} Buffering and Diffusion in Atrial Cardiac Myocytes with Inhibited Sarcoplasmic Reticulum, Biophys. J., 83 (2002), 3134–3151.

[18] G. D. Smith, J. E. Keizer, M. D. Stern, W. J. Lederer, and H. Cheng, A simple numerical model of calcium spark formation and detection in cardiac myocytes, Biophys. J., 75 (1998), 15–32.

[19] G. Dupont and C. Erneux, Simulations of the effects of inositol $1,4,5-$trisphosphate $3-$kinase and $5-$phosphatase activities on Ca^{2+} oscillations, Cell Calcium, 22 (1997), 321–331.

[20] A. Politi, L. D. Gaspers, A. P. Thomas, and T. Höfer, Models of IP_3 andCa^{2+} oscillations: frequency encoding and identification of underlying feedbacks, Biophys. J., 90 (2006), 3120–3133.

[21] J. Sneyd, K. Tsaneva-Atanasova, V. Reznikov, Y. Bai, M. J. Sanderson, and D. I. Yule, A method for determining the dependence of calcium oscillations on inositol trisphosphate oscillations, Proc. Nat. Acad. Sci., 103 (2006), 1675–1680.

[22] Y.-X. Li and J. Rinzel, Equations for $InsP_3$ Receptor-mediated $[Ca^{2+}]_i$ Oscillations Derived from a Detailed Kinetic Model: A Hodgkin-Huxley Like Formalism, J. Theor. Biol., 166 (1994), 461–473.

[23] G. W. De Young and J. Keizer, A single-pool inositol $1,4,5-$trisphosphate-receptor-based model for agonist-stimulated oscillations in Ca^{2+} concentration, Proc. Nat. Acad. Sci., 89 (1992), 9895–9899.

[24] X. Wu, T. Zhang, J. Bossuyt, X. Li, T. A. McKinsey, J. R. Dedman, E. N. Olson, J. Chen, J. H. Brown, and D. M. Bers, Local $InsP_3$-dependent perinuclear Ca^{2+} signaling in cardiac myocyte excitation-transcription coupling., J. Clinic. Invest., 116 (2006), 675–682.

[25] F. Hohendanner, A. D. McCulloch, L. A. Blatter, and A. P. Michailova, Calcium and IP_3 dynamics in cardiac myocytes: experimental and computational perspectives and approaches, Front. Pharmacol., 5 (2014), 1–15.

[26] N. L. Allbritton, T. Meyer, and L. Stryer, Range of messenger action of calcium ion and inositol $1,4,5-$trisphosphate, Science, 258 (1992), 1812–1814.

[27] J. Wagner, C. P. Fall, F. Hong, C. E. Sims, N. L. Allbritton, R. A. Fontanilla, I. I. Moraru, L. M. Loew, and R. Nuccitelli, A wave of IP_3 production accompanies the fertilization Ca^{2+} wave in the egg of the frog, Xenopus laevis: theoretical and experimental support, Cell Calcium, 35 (2004), 433–447.

[28] C. E. Sims and N. L. Allbritton, Metabolism of Inositol 1,4,5-Trisphosphate and Inositol 1,3,4,5-Tetrakisphosphate by the Oocytes of Xenopus laevis, J. Biol. Chem., 273 (1998), 4052–4058.

[29] N. Singh and N. Adlakha, Nonlinear Dynamic Modeling of 2-Dimensional Interdependent Calcium and Inositol 1,4,5-Trisphosphate in Cardiac Myocyte, Math. Biol. Bioinform., 14 (2019), 290–305.

[30] J. Sneyd, Calcium buffering and diffusion: on the resolution of an outstanding problem., Biophys. J., 67 (1994), 4-5.

[31] J. Wagner and J. Keizer, Effects of rapid buffers on Ca^{2+} diffusion and Ca^{2+} oscillations, Biophys. J., 67 (1994), 447–456.

[32] S. A. Brown, F. Morgan, J. Watras, and L. M. Loew, Analysis of phosphatidylinositol-4,5-bisphosphate signaling in cerebellar Purkinje spines, Biophys. J., 95 (2008), 1795–1812.

[33] C. C. Fink, B. Slepchenko, I. I. Moraru, J. Watras, J. C. Schaff, and L. M. Loew, An image-based model of calcium waves in differentiated neuroblastoma cells, Biophys. J., 79 (2000), 163–183.

[34] N. Singh and N. Adlakha, A mathematical model for interdependent calcium and inositol 1, 4, 5-trisphosphate in cardiac myocyte, Network Model. Anal. Health Inform. Bioinform., 8 (2019), 18.

[35] G. W. Recktenwald, Finite-Difference Approximations to the Heat Equation, Mech. Eng. 10 (2004), 1-27.

[36] K. B. Pathak and N. Adlakha, Finite Element Model to Study Calcium Signalling in Cardiac Myocytes Involving Pump, Leak and Excess Buffer, J. Med. Imaging Health Inform., 5 (2015), 683–688.

[37] P. J. Bartlett, W. Metzger, L. D. Gaspers, and A. P. Thomas, Differential Regulation of Multiple Steps in Inositol 1,4,5-Trisphosphate Signaling by Protein Kinase C Shapes Hormone-stimulated Ca^{2+} Oscillations, J. Biol. Chem., 290 (2015), 18519–18533.

[38] H.-J. Cho, H.-J. Cho, H.-J. Lee, M.-K. Song, J.-Y. Seo, Y.-H. Bae, J.-Y. Kim, H.-Y. Lee, W. Lee, B.-K. Koo, and Others, Vascular calcifying progenitor cells possess bidirectional differentiation potentials, PLoS Biol., 11 (2013), e1001534.

[39] K. Pathak and N. Adlakha, Finite Element Simulation of Advection Diffusion of Calcium in Myocyes Involving Influx and Excess Buffer, Adv. Comput. Sci. Technol., 10 (2017), 11–23.

[40] C. E. Adkins and C. W. Taylor, Lateral inhibition of inositol $1,4,5-$trisphosphate receptors by cytosolic Ca^{2+}, Current Biol., 9 (1999), 1115–1118.

[41] A. P. Dawson, Calcium signalling: How do IP_3 receptors work?, Current Biol., 7 (1997), R544–R547.

[42] T. J. Hund, A. P. Ziman, W. J. Lederer, and P. J. Mohler, The cardiac IP_3 receptor: Uncovering the role of "the other" calcium-release channel, J. Molecula Cellular Cardiol., 45 (2008), 159–161.

[43] J. Watras, B. E. Ehrlich, and Others, Bell-shaped calcium-response curves of $Ins(l,4,5)P_3$-and calcium-gated channels from endoplasmic reticulum of cerebellum, Nature, 351 (6329) (1991), 751–754.